Exploring processing, reactivity and performance of novel MAX phase/ultra-high temperature ceramic composites: the case study of Ti_3SiC_2

Laura Silvestroni[1*], Cesare Melandri[1], Jesus Gonzalez-Julian[2,3]

[1]*ISTEC-CNR, Via Granarolo 64, I-48018 Faenza (RA), Italy*

[2] *Forschungszentrum Jülich GmbH, Institute of Energy and Climate Research, Materials Synthesis and Processing (IEK-1), 52425 Jülich, Germany*

[3] *Chair of Ceramics and Refractory Materials, Institute of Mineral Engineering, RWTH Aachen University, 52064 Aachen, Germany*

Abstract

The reactivity behaviour between a MAX phase and ZrB_2 or WC was explored with the aim of developing novel composites by merging the benefits of the individual constituents. Hot pressing of Ti_3SiC_2 with 30 vol% ZrB_2 at 1450°C led to notable microstructure re-assessment with formation of inter-locked sub-micrometric boride grains. This composite displayed enhanced hardness and showed a strength over 430 MPa up to 1200°C, which is a great achievement considering the ductile behaviour of typical MAX compounds. However, addition of WC led to a highly porous composite with poor performance. These findings set a first basis for the progress of original light ceramics with combined hardness and failure tolerance over a broad temperature range.

Keywords: *MAX; borides; Hot pressing; mechanical properties; brittle-to-ductile-transition.*

Graphical abstract

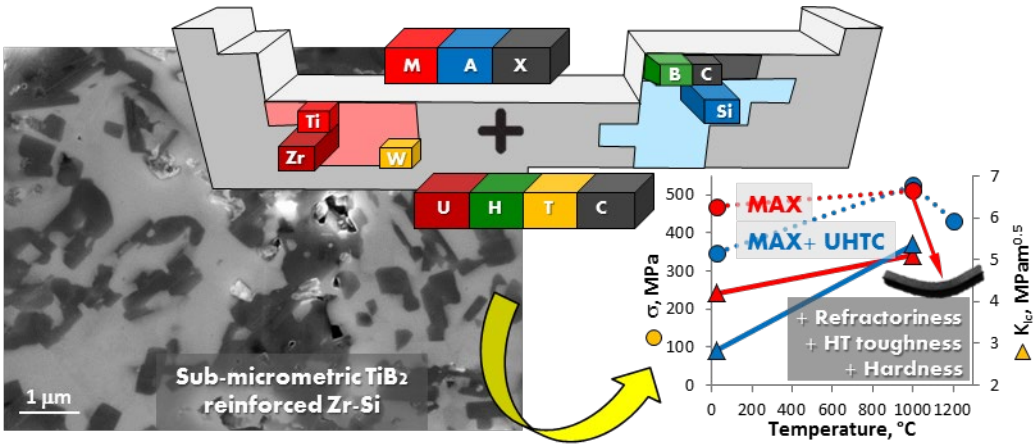

* Corresponding author: Laura Silvestroni
Via Granarolo 64, 48018 Faenza (Italy)
+39 546 699723
laura.silvestroni@istec.cnr.it

1. Introduction

MAX phases are promising candidates to operate under aggressive working conditions due to their unique combination of metallic and ceramic properties.[1,2] Among over 150 different compositions, Ti_3SiC_2 is the most studied compound due to the high elastic modulus (~ 340 GPa), compressive strength (~ 1050 MPa) and flexural strength (350-700 MPa) [2][3][4][5] coupled to remarkable fracture toughness achieving 16 MPa $m^{1/2}$.[6] This respectable value is combined with a nonlinear, hysterical, and elastic behaviour, which is highly unusual for stiff materials. [7] To note however that Ti_3SiC_2 undergoes a brittle-to-plastic-transition (BPT) around 1000°C, is relatively soft with hardness around 4 GPa, and other properties such as strength and creep should be improved to operate at high temperatures. In that sense Ti_3SiC_2 has been reinforced with different secondary phases. 40 vol% TiC particles increased the hardness of Ti_3SiC_2 to approx. 11 GPa, and the flexural strength from ~ 350 MPa to ~ 575 MPa.[8] SiC whiskers or particles have been also used to improve creep, contact damage resistance and hardness.[9],[10][11] However, elastic modulus and fracture toughness were just slightly enhanced and flexural strength notably decreased.

Better performance and operation ability extended to higher temperature ranges might be expected upon processing Ti_3SiC_2 with refractory ceramics such as Ultra High Temperature Ceramics (UHTCs). In this study, ZrB_2 or WC were selected as reinforcing phases in view of the melting point exceeding 3000°C of the first, and high hardness of the second. To the best of the authors' knowledge, processing of MAX phases with ZrB_2 and/or WC have not been reported yet and requires critical attention owing to the low stability of the MAX phases, with great tendency to dissociate into stable ceramic like SiC and TiC upon sintering at around 1400°C,[12] whereas UHTCs require sintering temperature in excess of 1800°C.[13]

The fundamental knowledge about the thermal stability of technologically important materials, like MAX phases is still very limited and the actual process of phase dissociation is poorly understood. This limited understanding has generated much debate. However, Ti_3SiC_2 is a relatively intensively studied phase, whose high-temperature thermo-chemical stability has been investigated in several works, all agreeing on the fact that it is susceptible to thermal dissociation at ~1400°C in inert environments (e.g., vacuum or argon) to form a surface TiC phase.[14–18] Presence of impuritites and oxides is expected to promote its dissociation by competing reactions.

This work explores the processing, interaction and resulting mechanical properties of novel MAX-UHTC composites with the aim of highlighting the critical aspects of combining two groups of compounds with such different reactivity and envisage the feasibility of novel compounds with possible evolving performance depending on the operating temperature.

2. Materials and methods

Ti_3SiC_2 powder (T-0) was synthesized by molten salt shielded synthesis route [11] and mixed with commercial ZrB_2 (H.C. Starck, Germany, #B) or WC (Treibacher Industries AG, Germany, #SD0.5) powders

through ball milling using SiC media for 24 h. Aware of the challenge of obtaining dense ceramics using the mild sintering conditions for preserving the MAX phase, we selected a percolating content equal to 30 vol% for ZrB_2 or WC, T-Z and T-W, respectively, Table I, to intentionally have clear evidence of the reaction products and possible evolution to completely new composites. The goal of this study was thus to highlight the processing limits of MAX-UHTC composites.

30 mm-diameter pellets were sintered in a low vacuum (~10 Pa) hot press with uniaxial pressure of 30 MPa, and a maximum temperature of 1300-1490°C, depending on the refractoriness of the mixture. During the isothermal dwell, 10-50 min, the pressure was increased to 40 MPa and then the furnace was turned off to cool naturally.

Since MAX phases are expected to dissociate at high temperature,[12,19] the actual density and porosity were calculated by mercury intrusion porosimetry (MIP) and ascertained by SEM inspection. Type and amount of crystalline phases were identified by x-ray diffraction (Bruker D8 Advance, Karlsruhe, Germany) on the as-synthesized Ti_3SiC_2 powder and on the polished cross-section of the sintered ceramics. The microstructure was analyzed on fractured and polished surfaces by scanning electron microscopy (FE-SEM, Carl Zeiss Sigma NTS Gmbh, Oberkochen, DE) and energy dispersive x-ray spectroscopy (EDS, INCA Energy 300, Oxford instruments, UK).

1kg Vickers microhardness (HV) was measured on polished surfaces using a standard indenter (Falcon 500 InnovaTest, The Netherlands). Bars for mechanical testing were cut from the sintered pellets by waterjet. The surface to be placed in tension was polished using a 30 μm diamond paste. Flexural strength (σ) at room temperature was measured according to the existing standard for advanced ceramics (ENV 843-1) on chamfered bars with 25 x 2.5 x 2.0 mm^3 length by width by thickness, respectively. Fracture toughness (K_{Ic}) was evaluated by chevron notched beam (CNB) method in flexure. The test bars with 25 mm x 2 mm x 2.5 mm length by width by thickness, respectively, were notched with a 0.1 mm-thick diamond saw; the chevron-notch tip depth and average side length were 0.12 and 0.80 of the bar thickness, respectively. The "slice model" equation of Munz et al.[20] was used to calculate K_{Ic}. Strength and toughness specimens were fractured using a fully-articulated four-point fixture with a lower span of 40 mm and an upper span of 20 mm using a screw-driven load frame (Instron, 6025).

For characterization up to 1200°C, specimens were fractured in flowing Ar in an Al_2O_3 4-point fixture after 18 soaking time to reach thermal equilibrium. For each material, property and temperature, three samples were tested. Young's modulus was estimated from the load-displacement curves once subtracted the compliance in the same load range.

3. Results and discussion

Fig. 1 shows the x-ray diffraction patterns of the starting T-0 powder and after hot pressing at 1300°C, where Ti_3SiC_2 as well as 10 vol% Al_2O_3 and TiC were detected. TiC amount passed from about 7 vol% in the

powder to more than 35 vol% after sintering, leaving only about 50 vol% of the original Ti_3SiC_2 phase in the dense pellet. SiC phase, deriving from Ti_3SiC_2 decomposition, was not detected given its low diffraction intensity, therefore, the phase composition reported in Table I is only indicative of the actual composition. Al_2O_3 is a typical by-product since the powders were synthesized in air with Al as catalyst.[21]

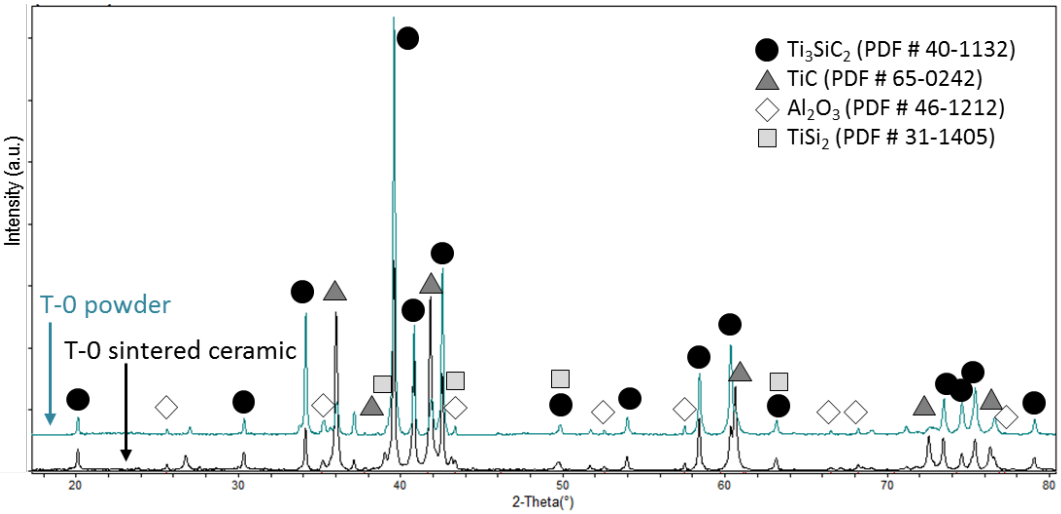

Fig. 1: XRD spectra of the Ti_3SiC_2 (T-0) starting powder and after hot pressing at 1300°C.

Table I: Composition, sintering parameters, experimental density, residual porosity and crystalline composition of the Ti_3SiC_2-based compounds as estimated by x-ray diffraction compared to an additive free Ti_3SiC_2 material sintered by SPS. [22]

Label	Additive, vol%	Sintering, °C/min/MPa	Exp. ρ, g/cm³	Pores by MIP, vol%	Phase composition by XRD, vol%
T	-	-		-	Ti_3SiC_2: 79.7, Al_2O_3: 13.5, TiC: 6.8
T-0	-	1300/50/40	4.22	3.3	Ti_3SiC_2: 49.5, TiC: 36.4, Al_2O_3: 8.6, $TiSi_2$:5.5
T-Z	30 ZrB_2	1450/10/40	4.05	13.2	TiC: 29.2, ZrSi: 25.8, TiB_2: 17.8, $ZrSi_2$: 14.6, (Zr,Ti)C: 6.5, Al_2O_3: 6.0
T-W	30 WC	1490/19/40	5.62	24.4	TiC: 55.1, Al_2O_3: 13.1, WC: 12.6, Ti_3SiC_2: 11.0, W_5Si_3: 6.1, WSi_2: 2.2
T-0[22]	-	1390/5/50	4.49	<1	TiC powder (KANTHAL, purity 99%)

The polished surface of T-0 sample is shown in Fig. 2a-c where a defect-free multiphasic microstructure can be appreciated. Al_2O_3 appears dark grey in BSE (Fig. 2a), or white in Inlens mode (Fig. 2b), image analysis revealed a content around 13 vol%, in agreement with XRD. In addition, SiC, TiC, $TiSi_2$, and residual Ti_3SiC_2 were confirmed by EDS analysis, however their relative amount was difficult to define given similar grey contrasts, Fig. 2bc. A porosity below 2% was also measured, in agreement with MIP.

Reactions involving MAX phase decomposition are:

$Ti_3SiC_2 \rightarrow 3TiC_{0.67} + Si(g)$ (1)

$Ti_3SiC_2 + 2C_{(g)} \rightarrow SiC + 3TiC$ (2)

$3Ti_3SiC_2 + 3C_{(g)} \rightarrow SiC + 8TiC + TiSi_2$ (3)

MAX decomposition is accompanied by pores formation owing to the volatilization of *A* species (Al or Si in this case), which have low vapor pressure and readily sublime above 1500°C.[12] Vaporization of Si might have caused the trapping of residual 2-3% porosity.

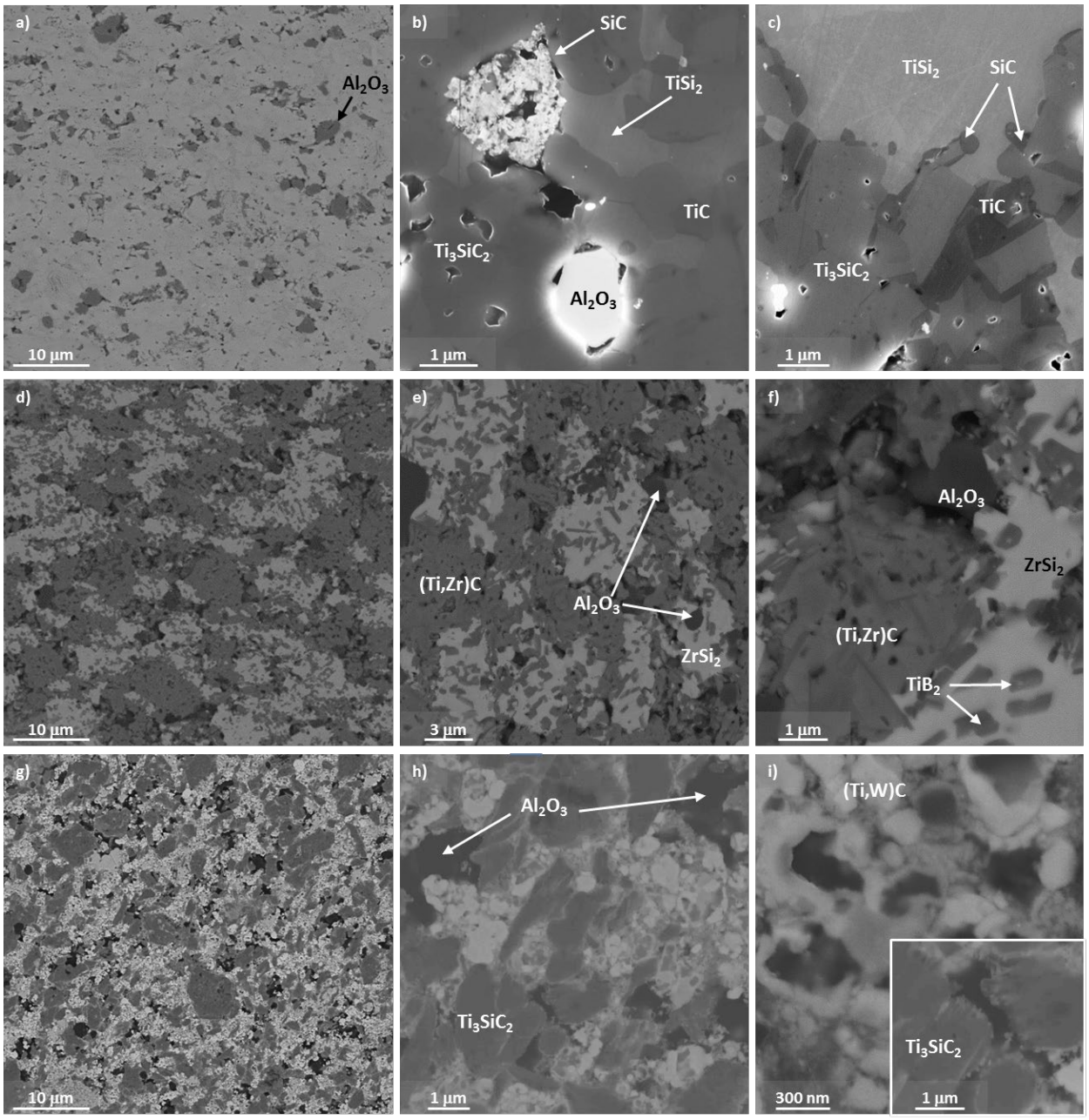

Fig. 2: SEM images of the polished surfaces of (a-c) T-0, (d-f) T-ZB and (g-i) T-WC ceramics showing microstructure overviews and magnifications of the phases formed upon sintering.

The crystallographic structure of the composite containing 30 vol% ZrB_2 (T-Z) became even more complex. Ti_3SiC_2 was not detected by XRD (inset in Fig. 3), but other reaction compounds such as TiC, ZrC, TiB_2, and Zr-silicides formed. ZrC peaks were found steadily shifted to higher 2-Theta angles, indicating a contraction of the unit cell, as illustrated in the inset of Fig. 3. This phenomenon has been already observed for analogous materials and is correlated with the formation of a (Zr,Ti)C solid solution where Ti with

smaller covalent radius substituted Zr larger atoms. 10 vol% of Al_2O_3 was present in this material too, suggesting that it did not take part in the reactive densification process.

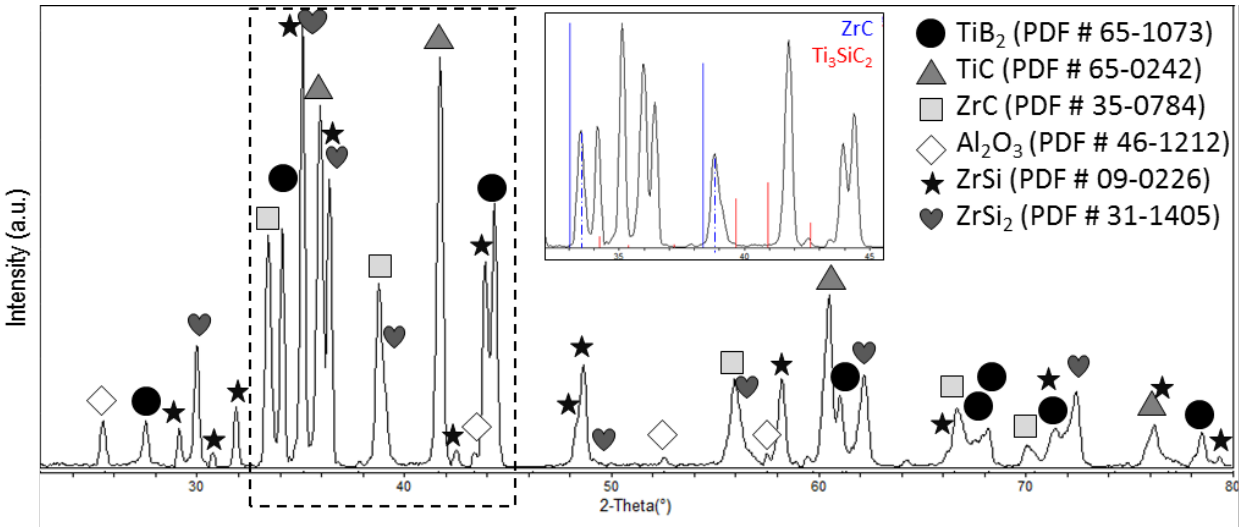

Fig. 3: XRD spectra of the Ti_3SiC_2 –ZrB_2 (T-Z) sintered pellet after hot pressing at 1450°C. The inset evidences disappearance of the Ti_3SiC_2 phase and ZrC peaks shift to higher 2-Theta angles.

SEM showed a porosity around 10 vol% and a multi-component spotted material. Besides Al_2O_3, two major phases could be identified in Fig. 2d-f: a grey one composed of acicular grains and based on (Zr,Ti)C and a bright one with ductile aspect and based on $ZrSi_2$. This phase systematically trapped dark nanosized rods identified by EDS to be TiB_2.

Plausible reactions for this microstructure evolution are:

$2Ti_3SiC_2 + 6ZrB_2 + C_{(g)} \rightarrow 6TiB_2 + ZrSi_2 + 5ZrC$ (4)

$2Ti_3SiC_2 + ZrB_2 + B_2O_3 + 3C_{(g)} \rightarrow 4TiC + 2TiB_2 + ZrSi_2 + 3CO(g)$ (5)

$TiC + ZrB_2 \rightarrow TiB_2 + ZrC$ (6)

Given the discrete amount of residual porosity in T-Z, 13.2 vol%, it is expected that reaction (5) is the most favourable, which yields volatile CO and TiB_2 and $ZrSi_2$ phases trapped into each other, Fig. 2f. Mutual solubility of Zr into TiC lattice is then favourable over a broad temperature range.[23]

Although the composite sintered with 30 vol% WC, T-W, was hot pressed at the highest temperature, 1490°C, 24.4 vol% porosity was left, Table I. This puts forward the hypothesis of gas development upon MAX decomposition in presence of reducing agents, in this case both the carbon-rich sintering environment and WC itself. According to XRD peaks intensity normalized over their RIR, the major phase was TiC, followed by WC and W-Silicides. Only about 10 vol% MAX phase was preserved after sintering and also in this case, about 13 vol% alumina was found, Fig. 4. SEM analysis (Fig. 2g-i) confirmed a complex microstructure asset, where the dark phases are Al_2O_3 and pores, the bright grey granulose phase is a mixed (Ti,W)-carbide, and the dark grey phase is residual Ti_3SiC_2. W-silicides had a bright grey aspect,

distinguishable from the carbides by a smoother texture, Fig. 2g. (Ti,W)C had sub-micrometric grains displaying the typical core-shell morphology with W enrichment in the outer region. In addition, MAX grains exhibited jagged edges suggesting progressive consumption (inset in Fig. 2i). Possible reactions between Ti_3SiC_2 and WC or its oxide are:

$3Ti_3SiC_2 + 5WC \rightarrow W_5Si_3 + 9TiC + 2C$ (7)

$3.75Ti_3SiC_2 + 5.25WC + WO_3 \rightarrow 1.25W_5Si_3 + 11.25TiC + 2.5CO_2$ (8)

$2Ti_3SiC_2 + WC + C \rightarrow WSi_2 + 6TiC$ (7)

$6Ti_3SiC_2 + WC + 2WO_3 + 11C \rightarrow 3WSi_2 + 18TiC + 6CO$ (9)

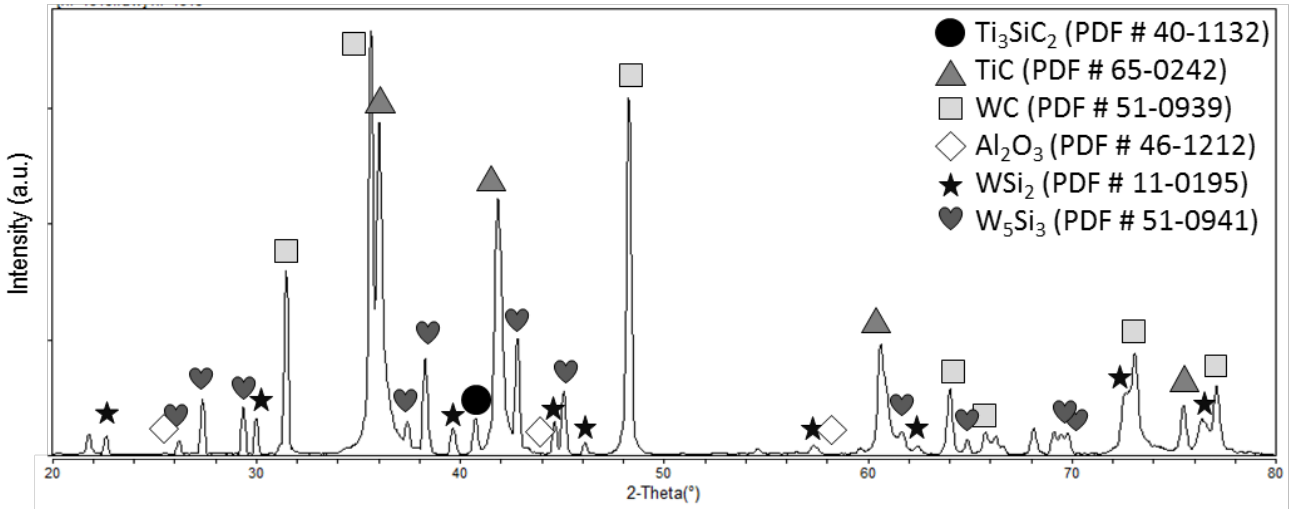

Fig. 4: XRD spectra of the Ti_3SiC_2 –WC (T-W) sintered pellet after hot pressing at 1490°C.

These microstructural investigations put forward the difficulty of MAX and UHTC coexistence, evidencing how ZrB_2 promoted the decomposition of Ti_3SiC_2 phase at 1450°C and formation of a completely different composite containing TiB_2 nanorods and Zr-carbides/silicides. On the other hand, upon addition of WC and sintering at 1490°C, residual Ti_3SiC_2 phase was left, but resulted in notable trapped porosity.

Improving approaches to eliminate the porosity and preserve the MAX phase include a decrease in the second phase amount, and consolidation by spark plasma sintering to decrease the maximum temperature and dwell time.[22]

Table II reports the mechanical properties of the Ti_3SiC_2–UHTC composites measured from room temperature to 1200°C in protective environment.

Vickers Hardness was strongly influenced by the residual porosity, however, the addition of ZrB_2 promoted a hardness increase from about 5.6 to 7.2 GPa, although having 10% porosity more than T-0. This suggests that formation of harder compounds, like TiB_2 and ZrC, in place of the soft Ti_3SiC_2 partially compensated the higher porosity. Stiffness suffered the residual porosity as well and ranged between 250-

280 GPa for the most dense composites, T-Z and T-0, and decreased to around 115 for T-W which contained more than 20% pores.

Material	HV, GPa	E, GPa	σRT, MPa	σ1000, MPa	σ1200, MPa	K_{Ic}RT, MPam$^{0.5}$	K_{Ic}1000, MPa·m$^{0.5}$	Ref.
T-0	5.6±0.3	282±24	470±40	512±58	bent	4.20±0.10	5.10±1.25	This work
T-Z	7.2±0.2	248±15	348±9	525±54	433±10	2.84±0.07	5.37±0.12	This work
T-W	2.6±0.1	117±28	172±4	185±36	94*	1.65±0.12	3.70±0.31	This work
Ti_3SiC_2	-	-	681±8	-	-	-	-	[22]
TiC	-	467±31	471±57	~370	~320	4.06±0.53	-	[24]
ZrC-ZrB_2-$MoSi_2$	12.5±0.9	390±4	363±31	-	256±119	4.0±0.9	-	[25]
ZrC-$MoSi_2$	19.2±0.4	-	474±41	-	330±62	3.42±0.45	-	[26]

*Just one bar tested given the poor performance

Table II: Microhardness (HV), Young's modulus (E), 4-point bending strength (σ), fracture toughness (K_{Ic}) at room and high temperature in Argon flux, measured for the Ti_3SiC_2-based compounds and compared to literature values.

Analogously, the room temperature strength decreased from about 470 MPa for T-0, to about 350 MPa for T-Z and down to around 170 MPa for the T-W composite. These values, although very reliable with low standard deviation, are generally lower than values reported in the literature [2][22] owing to the incomplete densification and partial or complete loss of the MAX phase. Looking at the fracture surfaces in Fig. 5a, Al_2O_3 had an intergranular fracture which brought out its globular aspect, whereas the silicide broke transgranularly. Magnified view of T-0 evidenced the fracture mode of the Ti_3SiC_2 phase featured by lamellar grains which pulled-out from the surface, Fig. 5b. Regarding the T-Z material, (Zr,Ti)C showed possible reminiscence of the Ti_3SiC_2 phase, with acicular sub-micrometric grains, whereas TiB_2 encapsulated into $ZrSi_2$ triggered a transgranular fracture across the silicide, Fig. 5d,e.

The fracture surface of T-W outlined the interconnected porosity and the weak grain boundaries between the newly formed carbides. Although they have a very fine granulometry, hundreds of nm, it is reasonable that TiC and WC did not densify well and remained with undeveloped necks among the particles at the low sintering temperature of 1490°C.

Testing the mechanical strength at 1000°C led to a general strength increase, suggesting healing of surface flaws, as visible in Fig. 5c,f,i, and the release of residual stresses deriving from coupling of different phases with different thermo-elastic properties. Little oxide formation was found on all composites given the weak

Ar flux in the hot chamber, Fig. 5c,f,i. ZrB_2 addition revealed its beneficial effect upon testing at 1000 and 1200°C, where the strength achieved about 525 and 430 MPa, respectively, providing an increase of above 50 and 24% as compared to its room temperature strength. Since the T-Z material mostly contained TiC, ZrC and ZrSi phases (Table I) a comparison with such ceramics would be more appropriate. The present T-Z MAX-UHTC composite overpassed the high temperature strength of a fully dense pure TiC material,[24] increasing by about 155 and 115 MPa upon testing at 1000 and 1200°C, respectively, owing to inhibition of TiC brittle-ductile transition temperature occurring at around 800°C.[27] Another positive hint towards the development of MAX-UHTC composites comes from the comparison of T-Z with ZrC-based materials,[25] where the present one displayed better strength than a pressureless sintered ZrC-ZrB_2-$MoSi_2$ material after bending strength at room and high temperature, overpassing the traditional UHTC composite by about 177 MPa at 1200°C in the same set-up and even behaved better than a hot pressed ZrC-$MoSi_2$ material that achieved only 330 MPa at 1200°C,[26] Table II. The better high-temperature strength behaviour of the T-Z material is probably related to the multi-scale length microstructure arrangement and the TiB_2 nanorods as strengthening phase.

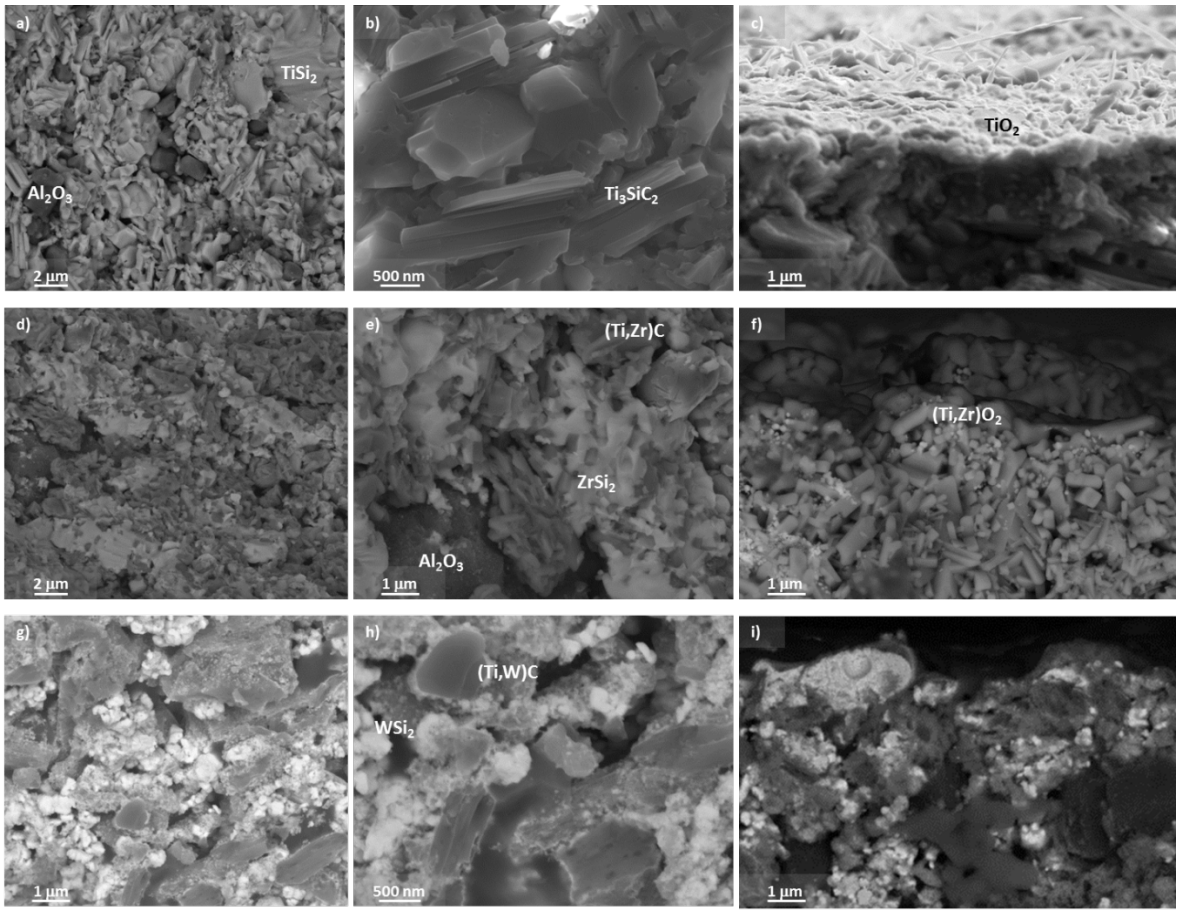

Fig. 5: SEM images of the fractured surfaces of (a-c) T-0, (d-f) T-ZB and (g-i) T-WC ceramics after bending test showing the fracture mode of the different phases at room temperature (left and central columns) and the oxide formed upon testing at 1000°C in partially protective environment (right column).

Moreover, if the pure Ti_3SiC_2 material bent once tested at 1200°C, the one containing ZrB_2 preserved the bar shape and a high strength. However, the addition of WC did not highlighted any benefits given the high residual porosity. Strength at 1000°C was in the same range as the room temperature one, whilst strength at 1200°C collapsed to 94.

Room temperature fracture toughness was influenced by the porosity and typical of brittle ceramics, without showing any MAX toughening contribution, ranging from 1.7 $MPa \cdot m^{0.5}$ for T-W to 4.2 $MPa \cdot m^{0.5}$ for T-0, with T-Z in-between. However, measures at 1000°C led to a general increase passing to 3.7 $MPa \cdot m^{0.5}$ for T-W, to 5.4 $MPa \cdot m^{0.5}$ for T-Z, which had comparable values as T-0, 5.1 $MPa \cdot m^{0.5}$. Although all bars maintained their shape, with no plastic behaviour macroscopically observed, this improvement is possibly due to the effect of some brittle-to-ductile transition of several of the phases constituting these composites, including silicides and residual MAX phase .

4. Conclusions

To explore the feasibility of MAX-UHTC composites with enhanced fracture behaviour, strength and hardness over a broad temperature range, a Ti_3SiC_2 phase was sintered with 30 vol% ZrB_2 or WC. Hot pressing at 1350-1490°C resulted in notable phase re-arrangement. When the boride was added, almost complete decomposition of the MAX phase occurred accompanied by formation of mixed (Zr,Ti)C phases and sub-micrometric TiB_2 rods interlocked into Zr-silicides. Sintering of MAX with WC, although decomposition was inhibited, led to notable trapped porosity that prevented achieving relevant mechanical performance. Overall, the MAX-ZrB_2 composite, despite possessing about 10 vol% porosity, improved the hardness of the unreinforced MAX baseline and achieved strength values that overpassed those of parent TiC- and ZrC-composites upon testing at 1000-1200°C, 525 and 430 MPa, respectively.

Acknowledgements

This work has been funded by the Germany´s Federal Ministry of Education and Research ("Bundesministerium für Bildung und Forschung") under the MAXCOM project (03SF0534). The authors would like to acknowledge Mr. Apurv Dash for his support on the synthesis process.

References

[1] B.M. Radovic, M.W. Barsoum, MAX phases : Bridging the gap between metals and ceramics, Am. Ceram. Soc. Bull. 92 (2013) 20–27.

[2] J. Gonzalez-Julian, Processing of MAX Phases: from synthesis to applications, J. Am. Ceram. Soc. (2021) in press. https://doi.org/10.1111/jace.17544.

[3] M.W. Barsoum, T. El-raghy, Synthesis and characterization of a remarkable ceramic Ti3SiC2, J. Am. Ceram. Soc. 79 (1996) 1953–1956.

[4] T. El-raghy, M.W. Barsoum, A. Zavaliangos, S.R. Kalidindi, Processing and mechanical properties of Ti3SiC2: II, Effect of Grain Size and deformation temperature, J. Am. Ceram. Soc. 82 (1999) 2855–2860.

[5] Z.M. Sun, Progress in research and development on MAX phases: a family of layered ternary compounds, Int. Mater. Rev. 56 (2011) 143–166. https://doi.org/10.1179/1743280410Y.0000000001.

[6] M.W. Barsoum, MAX Phases: Properties of Machinable Ternary Carbides and Nitrides, Wiley VCH, 2013.

[7] M.W. Barsoum, T. Zhen, S.R. Kalidindi, M. Radovic, A. Murugaiah, Fully reversible, dislocation-based compressive deformation of Ti3SiC2 to 1 GPa, Nat. Mater. 2 (2003) 107–111. https://doi.org/10.1038/nmat814.

[8] W. Tian, Z. Sun, H. Hashimoto, Y. Du, Synthesis, microstructure and mechanical properties of Ti3SiC2-TiC composites pulse discharge sintered from Ti/Si/TiC powder mixture, Mater. Sci. Eng. A. 526 (2009) 16–21.

[9] D. Wan, Y. Zhou, C. Hu, Y. Bao, Improved strength-impairing contact damage resistance of Ti3Si(Al)C2/SiC composites, J. Eur. Ceram. Soc. 27 (2007) 2069–2076. https://doi.org/10.1016/j.jeurceramsoc.2006.07.018.

[10] D.T. Wan, Y.C. Zhou, Y.W. Bao, C.K. Yan, In situ reaction synthesis and characterization of Ti3Si(Al)C2/SiC composites, Ceram. Int. 32 (2006) 883–890. https://doi.org/10.1016/j.ceramint.2005.07.004.

[11] A. Dash, J. Malzbender, K. Dash, M. Rasinski, R. Vassen, O. Guillon, J. Gonzalez-Julian, Compressive creep of SiC whisker/Ti3SiC2 composites at high temperature in air, J. Am. Ceram. Soc. 103 (2020) 5952–5965.

[12] I.-M. Low, An overview of parameters controlling the decomposition and degradation of Ti-Based Mn+1AXn phases, Materials (Basel). 12 (2019) 473. https://doi.org/10.3390/ma12030473.

[13] W.G. Fahrenholtz, E.J. Wuchina, W.E. Lee, Y. Zhou, eds., Ultra-High Temperature Ceramics: Materials for Extreme Environment Applications, John Wiley & Sons Inc., Hoboken, New Jersey, 2014. https://doi.org/10.1002/9781118700853.

[14] I.M. Low, Z. Oo, K.E. Prince, Effect of Vacuum Annealing on the Phase Stability of Ti3SiC2, J. Am. Ceram. Soc. 90 (2007) 2610–2614.

[15] Z. Oo, I.M. Low, B.H. O'Connor, Dynamic Study of the Thermal Stability of Impure Ti3SiC2 in Argon and Air by Neutron Diffraction, Phys. B. 385–386 (2006) 499–501.

[16] W.K. Pang, I.M. Low, Z.M. Sun, In Situ High-Temperature Diffraction Study of the Thermal

Dissociation of Ti3AlC2 in Vacuum, J. Am. Ceram. Soc. 93 (2010) 2871–2876.

[17] W.K. Pang, I.M. Low, B.H. O'Connor, A.J. Studer, V.K. Peterson, Z.M. Sun, J.-P. Palmquist, Effect of Vacuum Annealing on the Thermal Stability of Ti3SiC2/ TiC /TiSi2 Composite, J. Aust. Ceram. Soc. 45 (2009) 272–277.

[18] M. Griseri, B. Tunca, T. Lapauw, S. Huang, L. Popescu, M.W. Barsoum, K. Lambrinou, J. Vleugels, Synthesis, properties and thermal decomposition of the Ta4AlC3 MAX phase, J. Eur. Ceram. Soc. 39 (2019) 2973–2981.

[19] I. Low, W.K. Pang, Decomposition Kinetics of MAX Phases in Extreme Environments, in: I.M. Low, Y. Sakka, C.F. Hu (Eds.), MAX Phases Ultra-High Temp. Ceram. Extrem. Environ., IGI Global, United States, 2013: pp. 34–48. https://doi.org/10.4018/978-1-4666-4066-5.ch002.

[20] D.G. Munz, J.L.J. Shannon, R.T. Bubsey, Fracture toughness calculations from maximum load in four point bend tests of chevron notch specimens, Int. J. Fract. 16 (1980) R137–R141.

[21] Q. Wang, C. Hu, S. Cai, Y. Sakka, S. Grasso, Q. Huang, Synthesis of high-purity Ti3SiC2 by microwave sintering, Int J Appl Ceram Technol. 11 (2014) 911–918.

[22] M.A.Lagos, C. Pellegrini, I. Agote, N. Azurmendi, J. Barcena, M. Parco, L. Silvestroni, L. Zoli, D. Sciti, Ti3SiC2-Cf composites by spark plasma sintering: Processing, microstructure and thermo-mechanical properties, J. Eur. Ceram. Soc. 39 (2019) 2824–2830.

[23] H.O. Pierson, Handbook of Refractory Carbides and Nitrides, William Andrew Publishing, Norwich, NY, 2001.

[24] G.M. Song, Y.K. Guo, Y. Zhou, Q. Li, Preparation and mechanical properties of carbon fiber reinforced-TiC matrix composites, J. Mater. Sci. Lett. 20 (2001) 2157–2160.

[25] L. Silvestroni, D. Sciti, Microstructure and properties of pressureless sintered ZrC-based materials, J. Mater. Res. 23 (2008). https://doi.org/10.1557/jmr.2008.0234.

[26] L. Silvestroni, D. Sciti, Effect of transition metal silicides on microstructure and mechanical properties of ultra-high temperature ceramics, 2013. https://doi.org/10.4018/978-1-4666-4066-5.ch005.

[27] G. Das, K.S. Mazdiyasni, H.A. Lipsitt, Mechanical Properties of Polycrystalline TiC, J. Am. Ceram. Soc. 65 (1982) 104–110.

Tables

Table I: Composition, sintering parameters, experimental density, residual porosity and crystalline composition of the Ti_3SiC_2-based compounds as estimated by x-ray diffraction.

Label	Additive, vol%	Sintering, °C/min/MPa	Exp. ρ, g/cm³	Pores by MIP, vol%	Phase composition by XRD, vol%
T	-	-		-	Ti_3SiC_2: 79.7, Al_2O_3: 13.5, TiC: 6.8
T-0	-	1300/50/40	4.22	3.3	Ti_3SiC_2: 49.5, TiC: 36.4, Al_2O_3: 8.6, $TiSi_2$:5.5
T-Z	30 ZrB_2	1450/10/40	4.05	13.2	TiC: 29.2, ZrSi: 25.8, TiB_2: 17.8, $ZrSi_2$: 14.6, (Zr,Ti)C: 6.5, Al_2O_3: 6.0
T-W	30 WC	1490/19/40	5.62	24.4	TiC: 55.1, Al_2O_3: 13.1, WC: 12.6, Ti_3SiC_2: 11.0, W_5Si_3: 6.1, WSi_2: 2.2
T-0[22]	-	1390/5/50	4.49	<1	TiC powder (KANTHAL, purity 99%)

Table II: Microhardness (HV), Young's modulus (E), 4-point bending strength (σ), fracture toughness (K_{Ic}) at room and high temperature in Argon flux, measured for the Ti_3SiC_2-based compounds and compared to literature values.

Material	HV, GPa	E, GPa	σRT, MPa	σ1000, MPa	σ1200, MPa	K_{Ic}RT, MPam$^{0.5}$	K_{Ic}1000, MPa·m$^{0.5}$	Ref.
T-0	5.6±0.3	282±24	470±40	512±58	bent	4.20±0.10	5.10±1.25	This work
T-Z	7.2±0.2	248±15	348±9	525±54	433±10	2.84±0.07	5.37±0.12	This work
T-W	2.6±0.1	117±28	172±4	185±36	94*	1.65±0.12	3.70±0.31	This work
Ti_3SiC_2	-	-	681±8	-	-	-	-	[22]
TiC	-	467±31	471±57	~370	~320	4.06±0.53	-	[24]
ZrC-ZrB_2-$MoSi_2$	12.5±0.9	390±4	363±31	-	256±119	4.0±0.9	-	[25]
ZrC-$MoSi_2$	19.2±0.4	-	474±41	-	330±62	3.42±0.45	-	[26]

*Just one bar tested given the poor performance

Figure captions

Fig. 1: XRD spectra of the Ti_3SiC_2 (T-0) starting powder and after hot pressing at 1300°C.

Fig. 2: SEM images of the polished surfaces of (a-c) T-0, (d-f) T-ZB and (g-i) T-WC ceramics showing microstructure overviews and magnifications of the phases formed upon sintering.

Fig. 3: XRD spectra of the Ti_3SiC_2 –ZrB_2 (T-Z) sintered pellet after hot pressing at 1450°C. The inset evidences disappearance of the Ti_3SiC_2 phase and ZrC peaks shift to higher 2-Theta angles.

Fig. 4: XRD spectra of the Ti_3SiC_2 –WC (T-W) sintered pellet after hot pressing at 1490°C.

Fig. 5: SEM images of the fractured surfaces of (a-c) T-0, (d-f) T-ZB and (g-i) T-WC ceramics after bending test showing the fracture mode of the different phases at room temperature (left and central columns) and the oxide formed upon testing at 1000°C in partially protective environment (right column).